

Original Article

Impact of impaired cardiac function on the progression of chronic kidney disease—role of pharmacomodulation of valsartan

Chih-Chao Yang^{1*}, Hon-Kan Yip^{2,3,4,5,14*}, Kuan-Hung Chen⁶, Cheuk-Kwan Sun⁷, Yen-Ta Chen⁸, Han-Tan Chai², Pei-Hsun Sung², Hsin-Ju Chiang⁹, Sheung-Fat Ko¹⁰, Sheng-Ying Chung², Chih-Hung Chen¹¹, Kun-Chen Lin⁶, Pao-Yuan Lin¹², Jiunn-Jye Sheu¹³

¹Division of Nephrology, Department of Internal Medicine, Kaohsiung Chang Gung Memorial Hospital and Chang Gung University College of Medicine, Kaohsiung 83301, Taiwan, China; ²Division of Cardiology, Department of Internal Medicine, Kaohsiung Chang Gung Memorial Hospital and Chang Gung University College of Medicine, Kaohsiung 83301, Taiwan, China; ³Institute for Translational Research in Biomedicine, Kaohsiung Chang Gung Memorial Hospital, Kaohsiung, Taiwan, China; ⁴Center for Shockwave Medicine and Tissue Engineering, Kaohsiung Chang Gung Memorial Hospital, Kaohsiung, Taiwan, China; ⁵Department of Medical Research, China Medical University Hospital, China Medical University, Taichung 40402, Taiwan, China; ⁶Department of Anesthesiology, Kaohsiung Chang Gung Memorial Hospital and Chang Gung University College of Medicine, Kaohsiung 83301, Taiwan, China; ⁷Department of Emergency Medicine, E-Da Hospital, I-Shou University School of Medicine for International Students, Kaohsiung 82445, Taiwan, China; ⁸Division of Urology, Department of Surgery, Kaohsiung Chang Gung Memorial Hospital and Chang Gung University College of Medicine, Kaohsiung 83301, Taiwan, China; ⁹Department of Obstetrics and Gynecology, Kaohsiung Chang Gung Memorial Hospital and Chang Gung University College of Medicine, Kaohsiung 83301, Taiwan; ¹⁰Department of Radiology, Kaohsiung Chang Gung Memorial Hospital and Chang Gung University College of Medicine, Kaohsiung 83301, Taiwan; ¹¹Division of General Medicine, Department of Internal Medicine, Kaohsiung Chang Gung Memorial Hospital and Chang Gung University College of Medicine, Kaohsiung 83301, Taiwan; ¹²Division of Plastic and Reconstructive Surgery, Kaohsiung Chang Gung Memorial Hospital and Chang Gung University College of Medicine, Kaohsiung 83301, Taiwan; ¹³Division of Thoracic and Cardiovascular Surgery, Department of Surgery, Kaohsiung Chang Gung Memorial Hospital and Chang Gung University College of Medicine, Kaohsiung 83301, Taiwan; ¹⁴Department of Nursing, Asia University, Taichung 41354, Taiwan, China. *Equal contributors.

Received November 16, 2015; Accepted December 24, 2015; Epub May 15, 2017; Published May 30, 2017

Abstract: Although chronic kidney disease (CKD) is known to aggravate cardiovascular disease in the setting of cardiorenal syndrome (CRS), the impact of impaired cardiac function on the progression of CKD has seldom been reported. This study tested the impact of acute myocardial infarction on a rodent CKD model and the therapeutic effect of valsartan in this setting. Adult male Sprague-Dawley rats (n = 50) equally divided into group 1 (sham control), group 2 (CKD induced by 5/6 nephrectomy), group 3 (AMI by ligation of left coronary artery), group 4 (CKD+AMI), group 5 (CKD+AMI+valsartan, orally 10 mg/kg/day). By day 60, kidney injury score, creatinine levels, and ratio of urine to creatinine were highest in group 4 and lowest in group 1, significantly higher in group 4 than those in groups 2 and 5, and significantly higher in group 5 than those in group 2 (all p < 0.001). Protein expressions of inflammation (IL-1 β /MMP-9), oxidative stress (NOX-1/NOX-2/oxidized protein, angiotensin-II receptor), apoptosis (Bax, cleaved caspase-3/PARP), fibrosis (Smad3/TGF- β), and kidney injured (KIM-1/FSP-1) markers showed an identical pattern, whereas anti-fibrosis (Smad5/BMP-2) indices exhibited an opposite pattern compared to that of creatinine level among all groups (all p < 0.01). Cellular expressions of inflammation (CD14/CD68), DNA-damage (γ -H2AX, CD90/XRCC1) and proximal-renal tubule (KIM-1) biomarkers displayed an identical pattern, whereas podocyte-integrity markers (podocin/ZO-1/p-cadherin/synaptopodin) showed a pattern opposite to that of creatinine level among all groups (all p < 0.001). In a rodent CKD setting, renal function impairment and parenchymal damage further deteriorated after AMI but were suppressed following valsartan treatment.

Keywords: Chronic kidney disease, myocardial infarction, inflammation, oxidative stress, apoptosis, fibrosis

Introduction

Numerous studies have well established the fact that cardiovascular disease (CVD) [1, 2] and chronic kidney disease (CKD) [3-8] are two important predictors of unfavorable long-term outcome in different disease entities. A body of evidence has shown that organs of the body share information via a variety of biological mediators and pathology of one organ can lead to dysfunction of another [9]. Cardiorenal syndrome (CRS) is an important example of such an organ crosstalk. In fact, abundant data have demonstrated that CRS is a crucial factor in the prediction of short- and long-term prognostic outcomes in different disease settings [10-15]. In humans, the heart and the kidney are both considered major organs vital for survival. From the physiological standpoint, the heart acts as a pump that continuously provides adequate blood supply to the whole body. In situation of heart failure regardless of its etiology, the reduction in cardiac output decreases the blood flow to each organ, including the kidney, leading to a drop in glomerular filtration and impairment of renal function. On the other hand, the kidney is an important organ for metabolism, detoxification, and excretion of nitrogenous waste as well as the maintenance of pH, electrolyte, and fluid balance in our body. Accordingly, in situation of acute kidney injury or CKD, fluid and electrolyte imbalances as well as accumulation of uremic toxins contribute to impairment in endothelial and cardiac functions, thereby worsening cardiovascular disease. Therefore, it is rational to believe that CRS is the result of pathological crosstalk between the two organs. Surprisingly, while the adverse impact of CKD on the propagation of CVD in the setting of CRS has been keenly investigated, the possible damaging effects of heart dysfunction and CVD on renal function in the CKD setting receive much less attention. In view of the fact that CRS is one of the leading causes of death in hospitalized patients in different disease settings, the impact of cardiac dysfunction on renal function in the CKD setting warrants further clarification to guide clinical practice.

Accordingly, this study tested the hypothesis that (1) renal function would progressively deteriorate after acute myocardial infarction (AMI) in the setting of CKD, and (2) valsartan, which is a well-known angiotensin II type I receptor blocker for the treatment of patients with hypertension and CKD, would effectively pre-

vent the deterioration of renal function and molecular-cellular perturbations after AMI in a rodent model.

Materials and methods

Ethics

All animal experimental procedures were approved by the Institute of Animal Care and Use Committee at Kaohsiung Chang Gung Memorial Hospital (Affidavit of Approval of Animal Use Protocol No. 2013093004) and performed in accordance with the Guide for the Care and Use of Laboratory Animals [The Eighth Edition of the Guide for the Care and Use of Laboratory Animals (NRC 2011)].

Animals were housed in an Association for Assessment and Accreditation of Laboratory Animal Care International (AAALAC)-approved animal facility in our hospital with controlled temperature and light-dark cycle (24°C and 12/12 light-dark cycle).

Animal grouping and treatment strategy

Pathogen-free, adult male Sprague-Dawley (SD) rats (n = 50) weighing 325-350 g (Charles River Technology, BioLASCOTaiwan Co. Ltd., Taiwan) were randomly divided into five groups: sham-operated control (SC) (Group 1), CKD only (Group 2), AMI only (Group 3), CKD+AMI (CKD-AMI) (Group 4), CKD+AMI+valsartan orally 10 mg/kg/day since day 15 after CKD induction and up to end of the study period (i.e., at day 60 after CKD induction) (CKD-AMI-Val) (Group 5).

The dosage of valsartan use in the present study was based on our previous report with some modifications [16, 17].

Animal model of chronic kidney disease

The procedure and protocol of CKD was based on our recent report [18]. In details, all animals were anesthetized by inhalational 2.0% isoflurane in a supine position on a warming pad at 37°C for midline laparotomies. Sham-operated rats (SC) received laparotomy only, while CKD was induced in all animals in the CKD, CKD-AMI, and CKD-AMI-Va groups by right nephrectomy plus arterial ligation of upper two-third (i.e., upper and middle) blood supplies of the left kidney, leaving only blood supply to the lower third. Such a model allows preservation of limited amount of functioning renal parenchyma to simulate the condition of CKD.

Cardiac function affects CKD & modulated by valsartan

Animal model of AMI

The procedure and protocol of AMI induction were based on our recent reports [17, 19]. In details, by day 14 after CKD induction, all animals were anesthetized by inhalational 2.0% isoflurane and placed in a supine position on a warming pad at 37°C. Under sterile conditions, the heart was exposed via a left thoracotomy. Sham-operated rats (SC) received thoracotomy only, while AMI was induced in AMI, AMI-CKD and AMI-CKD-Val animals by left coronary artery ligation 3 mm distal to the margin of left atrium with 7-0 prolene suture. Regional myocardial ischemia was verified by observing a rapid color change from pinkish to dull red-dish over the anterior surface of the LV and rapid development of akinesia and dilatation in the ischemic region. After the procedure, the thoracotomy wound was closed and the animals were allowed to recover from anaesthesia in a portable animal intensive care unit (ThermoCare®) for 24 hours.

Functional assessment by echocardiography

All animals underwent transthoracic echocardiography under general anesthesia in supine position at the beginning and end of the study. The procedure was performed by an animal cardiologist blinded to the experimental design using an ultrasound machine (Vevo 2100, Visualsonics). Standard M-mode two-dimensional (2D) left parasternal-long axis echocardiographic examination was conducted. Left ventricular internal dimensions, including end-systolic diameter (ESD) and end-diastolic diameter (EDD), were measured according to the American Society of Echocardiography leading-edge method using at least three consecutive cardiac cycles. Left ventricular ejection fraction (LVEF) was calculated as follows: $LVEF (\%) = [(LVEDD^3 - LVEDS^3) / LVEDD^3] \times 100\%$.

Abdominal ultrasonography for determining renal blood flow

The procedure and protocol of abdominal ultrasonographic measurement was based on our recent report [18]. Briefly, for abdominal ultrasound examination, the animals in each group were anesthetized with inhalational 2.0% isoflurane on days 0, 14 and 60 prior to be sacrificed. After shaving of the abdominal in all animals, abdominal sonography (Vevo 2100, Visual Sonics Inc., Toronto, Canada) was per-

formed by an experienced technician blinded to the treatment protocol. The renal blood flow/velocity and color Doppler signals were carefully measured three times in each rat. The parameters were averaged and entered into a computer for further analysis.

Assessment of blood urea nitrogen (BUN) and creatinine levels

The blood samples were collected before and after the CKD procedure (i.e., prior to and at day 60) before being sacrificed for assessment of serum creatinine and BUN levels were performed in the present study. The procedure and protocol for measuring these parameters have been reported in our recent study [18] in details. In briefly, the concentrations of serum creatinine and BUN were measured in duplicate using standard laboratory equipment. The mean intra-assay coefficient of variance for BUN and creatinine was less than 4.0%.

Collection of 24-Hour urine for the ratio of urine protein to creatinine at days 14 and 60 after CKD induction

For determining whether the CKD was successful induction and the impact of valsartan on protecting the renal function in CKD-AMI setting, the urine in 24 hrs of all animals were collected and the ratio of urine protein to creatinine was determined at days 14 and 60 after CKD induction. For the collection of 24-hr urine for individual study, each animal was put into a metabolic cage [DXL-D, space: 190 x 290 x 550, Suzhou Fengshi Laboratory Animal Equipment Co. Ltd., Mainland China] for 24 hrs with free access to food and water.

Histopathology scoring of kidney injury

The histopathology scoring of kidney injury was determined in a blinded fashion as we previously reported [19-21]. Briefly, the left kidney specimens from all animals were fixed in 10% buffered formalin, embedded in paraffin, sectioned at 4 µm and stained (hematoxylin and eosin; H&E) for light microscopy. The score reflected the grading of tubular necrosis, loss of brush border, cast formation, tubular dilatation, and Bowman's capsule enlargement in 10 randomly chosen, non-overlapping fields (200x) for each animal as follows: 0 (none), 1 (≤ 10%), 2 (11-25%), 3 (26-45%), 4 (46-75%), and 5 (≥ 76%).

Cardiac function affects CKD & modulated by valsartan

Determined the distribution of small vessels in kidney parenchyma

The detailed procedure and protocol for determining the number of small vessel have been described in our previous reports [22, 23]. Briefly, immunohistochemical (IHC) staining of α -smooth muscle actin using the appropriate antibodies (Sigma) was performed to identify renal arterioles according to manufacturer's instructions. Three kidney sections from each rat were analyzed and three randomly selected HPFs (100x) were analyzed in each section. The mean number per HPF for each animal was then determined by summation of all numbers divided by 9.

Measurement of arterial muscularization in kidney parenchyma

The detailed procedure and protocol for determining muscularization (i.e., an index of vascular remodeling) of renal arterioles was based on our previous report [23]. Briefly, three measurements were taken for the thickness of renal arterioles. Muscularization of the arterial medial layer in renal parenchyma was defined as a mean thickness of vessel wall greater than 50% of the lumen diameter in a vessel of diameter > 30 μ m. Measurement of arteriolar diameter and wall thickness was achieved using the Image-J software (NIH, Maryland, USA).

Western blot analysis of right kidney specimens

The methods were previously described in details in our recent reports [16-21]. Primary antibodies against angiotensin II receptor (1:1000, Abcam), fibroblast specific protein 1 (FSP-1) (1:1000, Abcam), Wilm's tumor suppressor gene 1 (WT-1) (1:1000, Abcam), kidney injury molecule (KIM)-1 (1:500, Abcam), matrix metalloproteinase (MMP)-9 (1:1000, Millipore), interleukin (IL)-1 β (1:1000, Abcam), NADPH oxidase (NOX)-1, 2 (1:1500, Sigma), caspase 3 (1:1000, Cell Signaling), poly (ADP-ribose) polymerase (PARP) (1:1000, Cell Signaling), Smad3 (1:1000, Cell Signaling), Smad1/5 (1:1000, Cell Signaling), transforming growth factor (TGF)- β (1:500, Abcam), bone morphogenetic protein (BMP)-2 (1:500, Abcam), Bcl-2 (1:200, Abcam), phospho-Akt (1:1000, Cell Signaling) were used. Signals were detected with horseradish peroxidase (HRP)-conjugated goat anti-mouse, goat anti-rat, or goat anti-rabbit IgG. Immunoreactive bands were visualized by

enhanced chemiluminescence (ECL; Amersham Biosciences), which was then exposed to Biomax L film (Kodak). For quantification, ECL signals were digitized using Labwork software (UVP).

Immunohistochemical and immunofluorescent studies

The procedures and protocols for immunohistochemical (IHC) and immunofluorescent (IF) examinations were based on our recent studies [16-21]. For IHC and IF staining, rehydrated paraffin sections were first treated with 3% H₂O₂ for 30 minutes and incubated with Immuno-Block reagent (BioSB) for 30 minutes at room temperature. Sections were then incubated with primary antibodies specifically against CD68 (1:100, Abcam), CD14 (1:200, BioSS), γ -H2AX (1:500, Abcam), CD90/XRCC1 (1:100, Abcam/1:200, Abcam), zonula occludens-1 (ZO-1) (1:300, Abcam), kidney injury molecule (KIM)-1 (1:200, R&D system), p-cadherin (1:100, Novus), podocin (1:100, Sigma), and synaptopodin (1:100, Santa Cruz) while sections incubated with the use of irrelevant antibodies served as controls. Three sections of kidney specimens were analyzed in each rat. For quantification, three randomly selected HPFs (x200 for IHC and IF studies) were analyzed in each section. The mean number per HPF for each animal was then determined by summation of all numbers divided by 9. An IHC-based scoring system was adopted for semi-quantitative analyses of ZO-1 p-cadherin, podocin, KIM-1, and synaptopodin in the kidneys as a percentage of positive cells in a blinded fashion (score of positively-stained cell for these biomarkers: 0 = negative staining; 1 \leq 15%; 2 = 15-25%; 3 = 25-50%; 4 = 50-75%; 5 \geq 75%-100% per HPF).

Assessment of oxidative stress

The Oxyblot Oxidized Protein Detection Kit was purchased from Chemicon, Billerica, MA, USA (S7150). DNPH derivatization was carried out on 6 μ g of protein for 15 minutes according to the manufacturer's instructions. One-dimensional electrophoresis was carried out on 12% SDS/polyacrylamide gel after DNPH derivatization. Proteins were transferred to nitrocellulose membranes which were then incubated in the primary antibody solution (anti-DNP 1:150) for 2 hours, followed by incubation in secondary antibody solution (1:300) for 1 hour at room temperature. The washing procedure was re-

Cardiac function affects CKD & modulated by valsartan

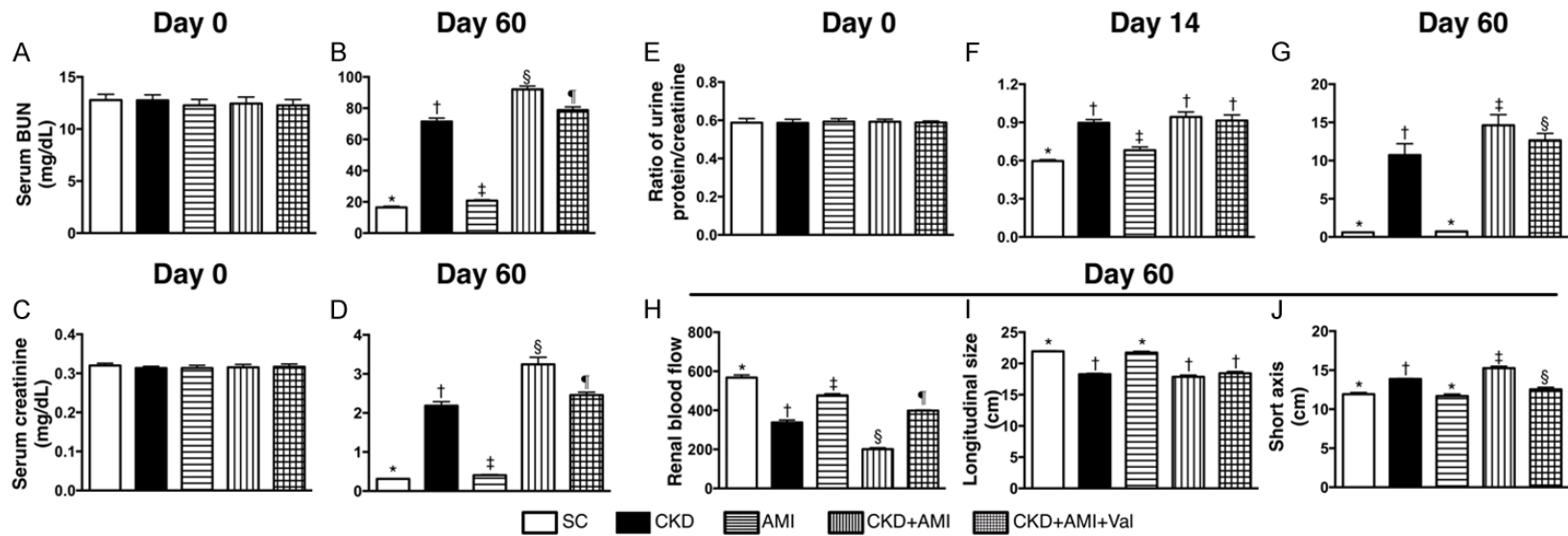


Figure 1. Measurement of serum levels of creatinine and blood urea nitrogen (BUN), the ratio of urine protein to creatinine, renal blood flow and kidney size. A. Serum level of creatinine by day 0 prior to CKD induction, * vs. other groups, $p > 0.5$. B. Serum level of creatinine by day 60 after CKD, * vs. other groups with different symbols (†, ‡, §, ¶), $p < 0.0001$. C. Serum level of BUN by day 0 prior to CKD induction, * vs. other groups, $p > 0.5$. D. Serum level of BUN by day 60 after CKD, * vs. other groups with different symbols (†, ‡, §, ¶), $p < 0.0001$. E. Ratio of urine protein to creatinine by day 0 prior to CKD induction, * vs. other groups, $p > 0.5$. F. Ratio of urine protein to creatinine by day 16 after CKD induction prior to AMI induction, * vs. † $p < 0.001$. G. Ratio of urine protein to creatinine by day 60 after CKD, * vs. other groups with different symbols (†, ‡, §), $p < 0.0001$. H. Renal blood flow velocity by day 60 after CKD induction, * vs. other groups with different symbols (†, ‡, §, ¶), $p < 0.0001$. I. Long axis of kidney by day 60 after CKD induction, * vs. † $p < 0.0001$. J. Short axis of kidney by day 60 after CKD induction, * vs. other groups with different symbols (†, ‡, §), $p < 0.0001$. All statistical analyses were performed by one-way ANOVA, followed by Bonferroni multiple comparison post hoc test ($n = 10$). Symbols (*, †, ‡, §, ¶) indicate significance (at 0.05 level). Scale bars in right lower corner represent 50 μm . SC = sham control; AMI = acute myocardial infarction; CKD = chronic kidney disease; Val = valsartan.

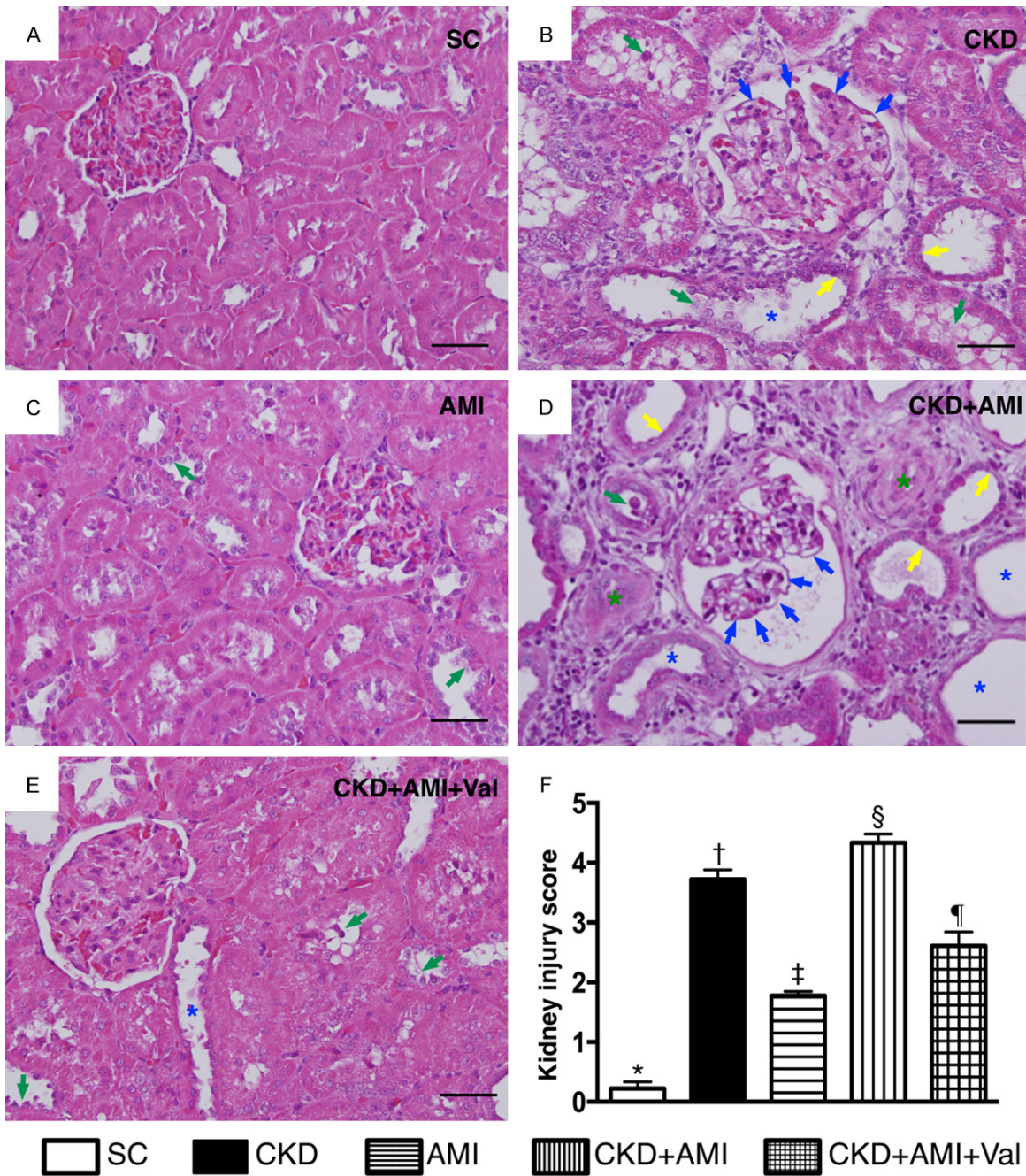


Figure 2. Histopathological findings of kidney injury by day 60 after CKD induction. A-E. H&E. stain (400x) demonstrating significantly higher degree of loss of brush border in renal tubules (yellow arrows), cast formation (green asterisk), tubular dilatation (blue asterisk) tubular necrosis (green arrows), and dilatation of Bowman's capsule (blue arrows) in CKD and CKD+AMI groups than in other groups. F. * vs. other groups with different symbols (†, ‡, §, ¶), * vs. †p < 0.0001. All statistical analyses were performed by one-way ANOVA, followed by Bonferroni multiple comparison post hoc test (n = 10). Symbols (*, †, ‡, §, ¶) indicate significance (at 0.05 level). Scale bars in right lower corner represent 50 µm. SC = sham control; AMI = acute myocardial infarction; CKD = chronic kidney disease; Val = valsartan.

peated eight times within 40 minutes. Immuno-reactive bands were visualized by enhanced chemiluminescence (ECL; Amersham Biosci-

ces, Amersham, UK) which was then exposed to Biomax L film (Kodak, Rochester, NY, USA). For quantification, ECL signals were digitized

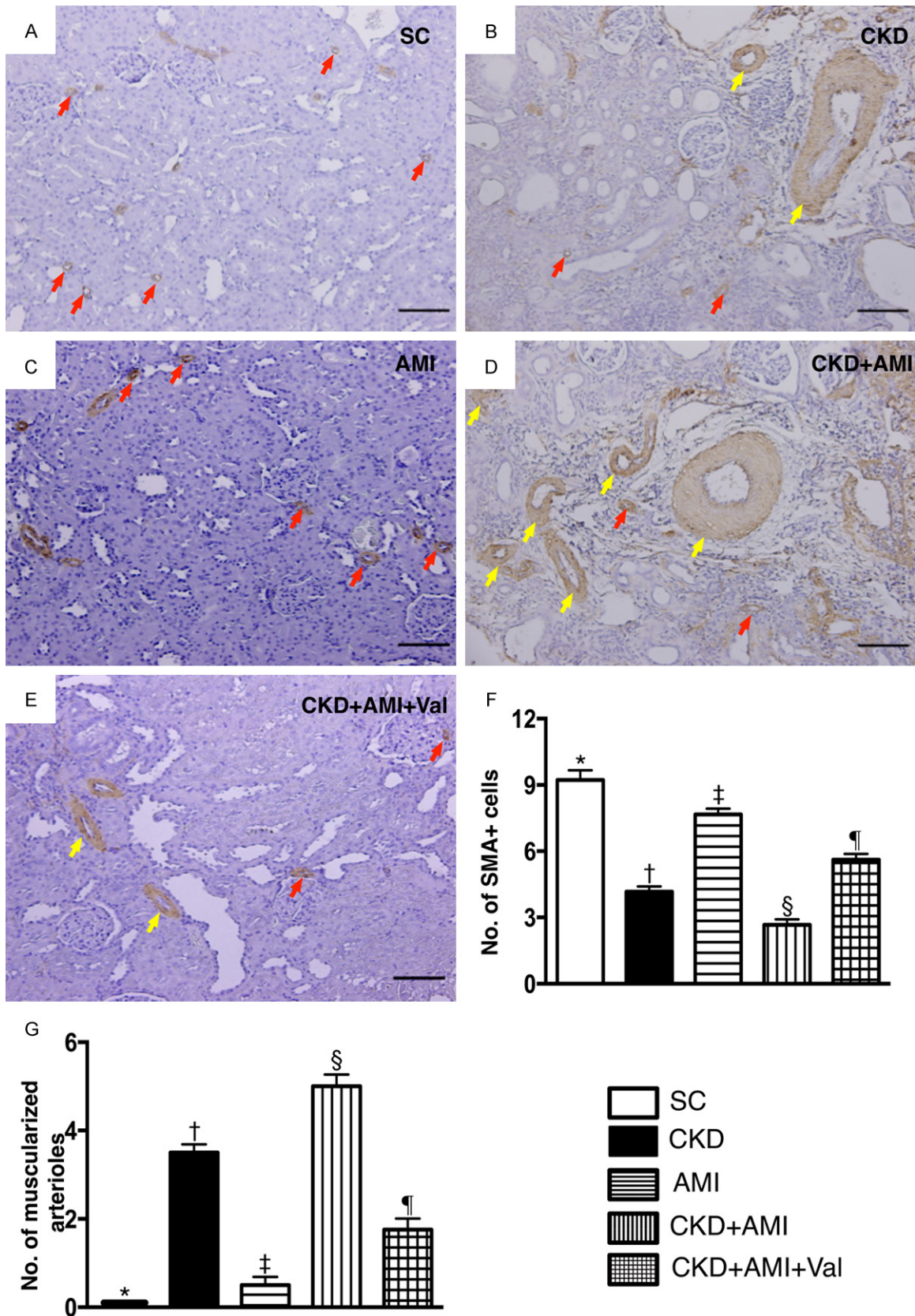


Figure 3. Numbers of small vessels and arterial muscularization in kidney parenchyma by day 60 after CKD induction. A-E. Illustration of the microscopic findings (100x) of immunohistochemical staining (i.e., α -smooth muscle

Cardiac function affects CKD & modulated by valsartan

actin) for identification of numbers of small vessels (red arrows) and the arterial muscularization (yellow arrows). F. Statistical analysis of the number of small vessels, * vs. other groups with different symbols (†, ‡, §, ¶), $p < 0.0001$. G. Statistical analysis of the number of muscularization, * vs. other groups with different symbols (†, ‡, §, ¶), $p < 0.0001$. All statistical analyses were performed by one-way ANOVA, followed by Bonferroni multiple comparison post hoc test ($n = 10$). Symbols (*, †, ‡, §, ¶) indicate significance (at 0.05 level). Scale bars in right lower corner represent 100 μm . SC = sham control; AMI = acute myocardial infarction; CKD = chronic kidney disease; Val = valsartan.

using Labwork software (UVP, Waltham, MA, USA). For oxyblot protein analysis, a standard control was loaded on each gel.

Statistical analysis

Quantitative data are expressed as means \pm SD. Statistical analyses were performed using SAS statistical software for Windows version 8.2 (SAS institute, Cary, NC) to conduct ANOVA, followed by Bonferroni multiple-comparison post hoc test. A probability value < 0.05 was considered statistically significant.

Results

Blood urea nitrogen (BUN) and creatinine levels prior to and after CKD induction, and ultrasound findings of the kidneys by day 60 after CKD induction (Figure 1)

By day 0 prior to CKD induction, the serum levels BUN and creatinine, and the ratio of urine protein to creatinine did not differ among the five groups. However, by day 60 after CKD induction, these three parameters were highest in CKD-AMI and lowest in SC, significantly higher in CKD than those in AMI and CKD-AMI-Val, and significantly higher in CKD-AMI-Val than those in the AMI group. Additionally, by day 14 after CKD induction and prior to AMI induction, the ratio of urine protein to creatinine were significantly higher in CKD, CKD-AMI and CKD-AMI-Val groups than in SC and AMI groups, but this parameter did not differ among the former three groups or between the later two groups. Furthermore, by day 60 after CKD induction, the ratio of urine protein to creatinine were highest in CKD-AMI and lowest in SC and AMI, and significantly higher in CKD than in CKD-AMI-Val, but it showed no difference between SC and AMI.

Renal ultrasonography showed that, prior to the procedure (i.e., day 0), the kidney size was similar among the five groups. However, by day 60 after the CKD induction, the short axis of kidney was shortest in AMI-CKD and longest in SC and AMI, and significantly shorter in CKD than that in CKD-AMI-Va, but it showed no difference bet-

ween SC and AMI animals. On the other hand, the pattern of changes in the long axis of kidney was significantly shorter in AMI-CKD than in other groups, significantly shorter in CKD and AMI-CKD-Va than in SC and AMI, but it showed no difference between the former two groups or between the later two groups.

On the other hand, renal blood flow was highest in SC and lowest in AKD-AMI, significantly reduced in CKD compared to that in AMI and CKD-AMI-Va, and significantly lower in AMI-CKD-Va than that in the AMI group.

Histological damage in kidney parenchyma by day 60 after CKD induction (Figure 2)

H&E staining of left kidney sections revealed that the kidney injury score was highest in CKD-AMI and lowest in SC, significantly higher in CKD than that in AMI and CKD-AMI-Val, and significantly higher in CKD-AMI-Val than that in the AMI animals. Accordingly, the findings suggest that AMI worsened renal function that was preserved by valsartan therapy in the experimental setting of CKD.

Distribution of small vessels and histological finding of arterial muscularization in kidney parenchyma by day 60 after CKD induction (Figure 3)

IHC staining of α -smooth muscle actin demonstrated that the number of small vessels in renal parenchyma was lowest in CKD-AMI and highest in SC, significantly lower in CKD than that in AMI and CKD-AMI-Val, and significantly lower in CKD-AMI-Val than that in animals with AMI only. On the other hand, the number of arterial muscularization in kidney parenchyma exhibited an opposite pattern compared to that of the number of small vessels among the five groups.

Immunohistochemical and immunofluorescent analyses of podocytes in glomeruli by day 60 after CKD induction (Figures 4 and 5)

IF analysis showed that the expression of ZO-1 (Figure 4), a tight junction-associated protein

Cardiac function affects CKD & modulated by valsartan

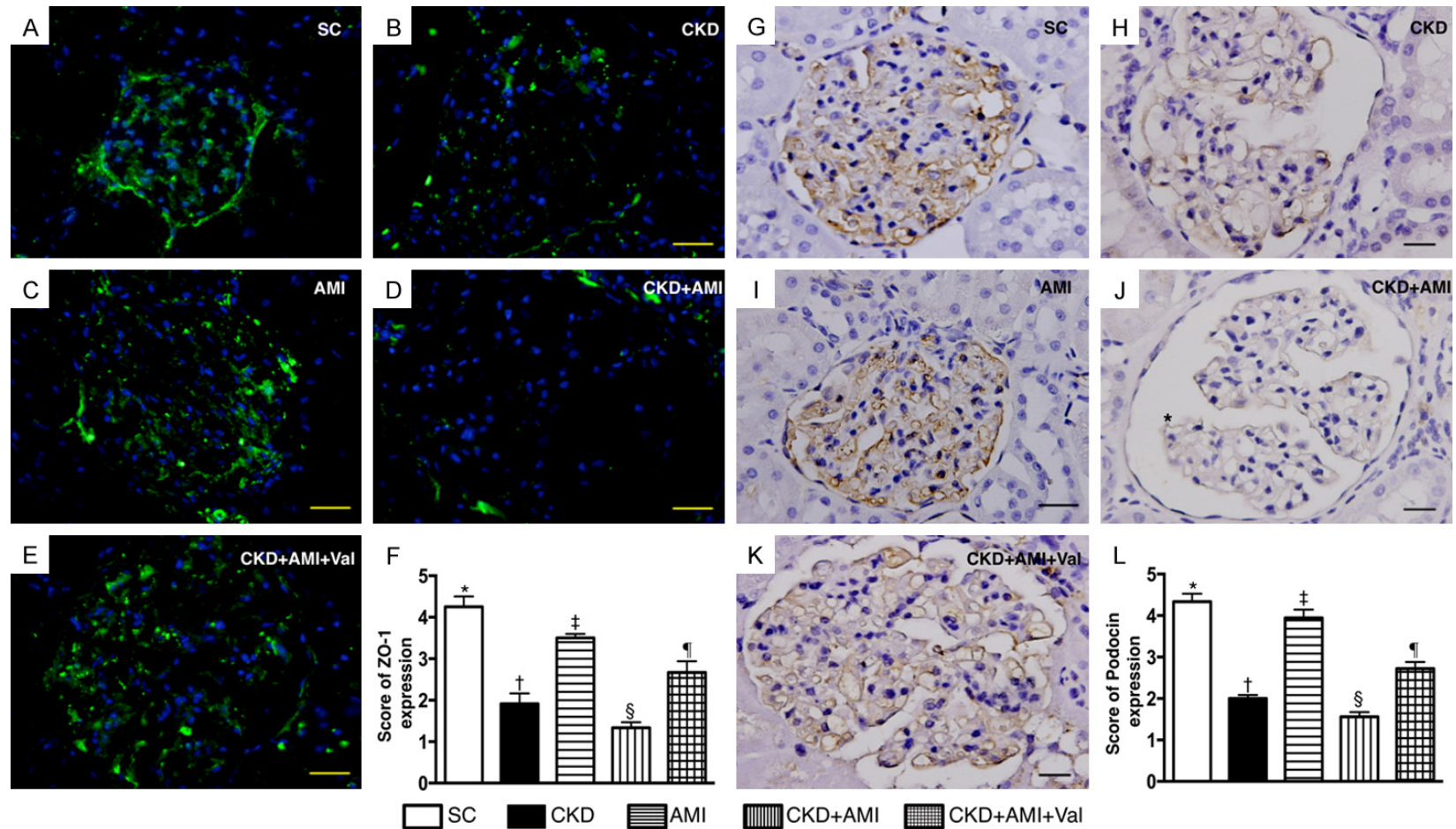


Figure 4. Immunofluorescent (IF) stain for identification of zonula occludens-1 (ZO-1) and Immunohistochemical (IHC) stain for assessment of podocin by day 60 after CKD induction. A-E. Illustrating the microscopic finding (400x) of IF staining for identification of zonula occludens-1 (ZO-1) in renal glomerulus (green color). F. Analytical results of ZO-1 expression, * vs. other groups with different symbols (†, ‡, §, ¶), $p < 0.0001$. Scale bars in right lower corner represent 20 μ m. G-K. Illustrating the microscopic finding (200x) of IHC staining for assessment of podocin in renal glomerulus (gray color). L. * vs. other groups with different symbols (†, ‡, §, ¶), $p < 0.0001$. Scale bars in right lower corner represent 20 μ m. All statistical analyses were performed by one-way ANOVA, followed by Bonferroni multiple comparison post hoc test ($n = 10$). Symbols (*, †, ‡, §, ¶) indicate significance (at 0.05 level). SC = sham control; AMI = acute myocardial infarction; CKD = chronic kidney disease; Val = valsartan.

Cardiac function affects CKD & modulated by valsartan

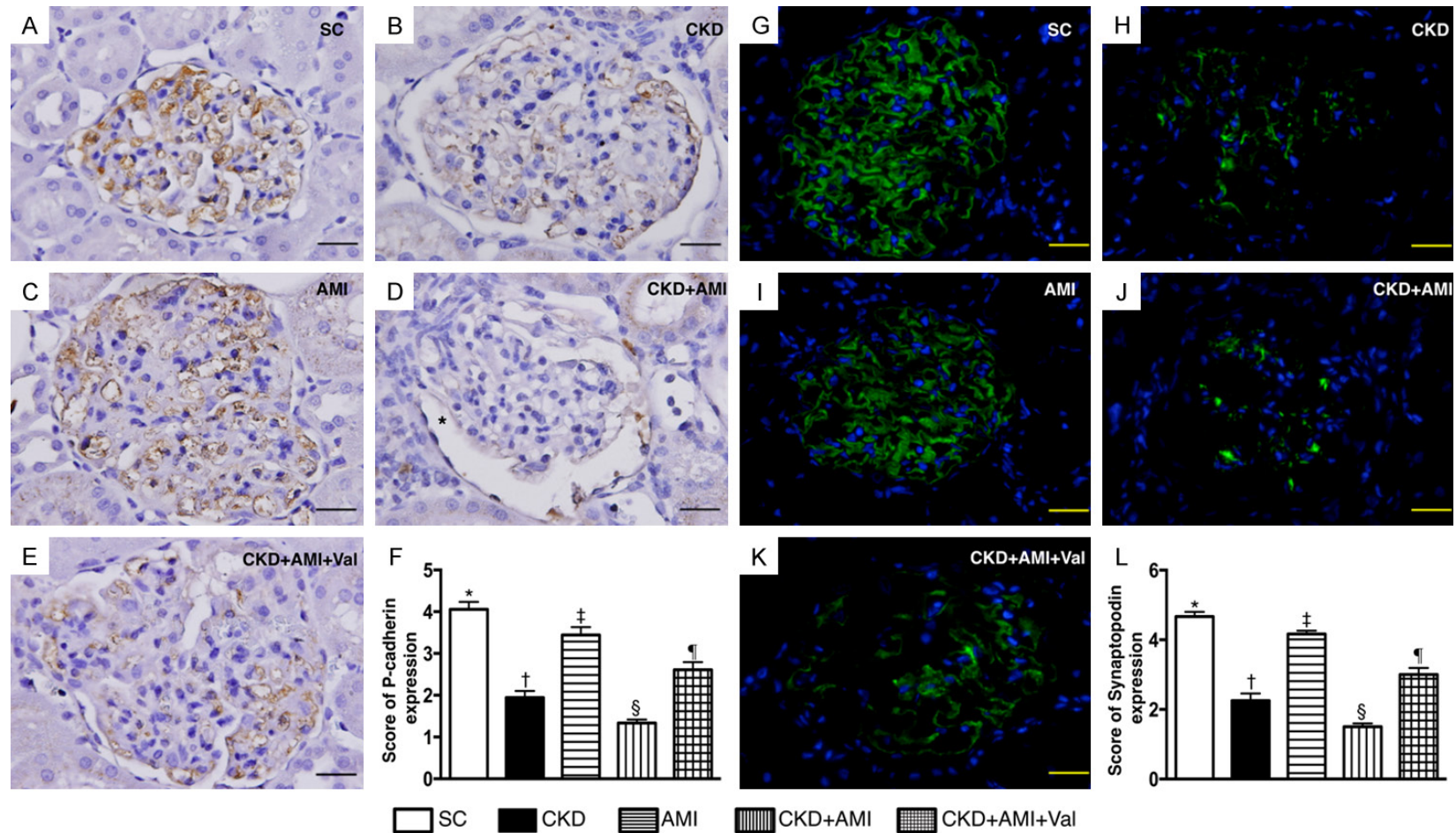


Figure 5. Immunohistochemical (IHC) stain for assessment of P-cadherin and Immunofluorescent (IF) stain for identification of synaptopodin by day 60 after CKD induction. A-E. Illustrating the microscopic finding (400x) of IHC staining for identification of P-cadherin in renal glomerulus (gray color). F. Analytical results of P-cadherin expression, * vs. other groups with different symbols (†, ‡, §, ¶), $p < 0.0001$. Scale bars in right lower corner represent 20 μm . G-K. Illustrating the microscopic finding (400x) of IF staining for assessment of synaptopodin in renal glomerulus (green color). L. * vs. other groups with different symbols (†, ‡, §, ¶), $p < 0.0001$. Scale bars in right lower corner represent 20 μm . All statistical analyses were performed by one-way ANOVA, followed by Bonferroni multiple comparison post hoc test ($n = 10$). Symbols (*, †, ‡, §, ¶) indicate significance (at 0.05 level). SC = sham control; AMI = acute myocardial infarction; CKD = chronic kidney disease; Val = valsartan.

Cardiac function affects CKD & modulated by valsartan

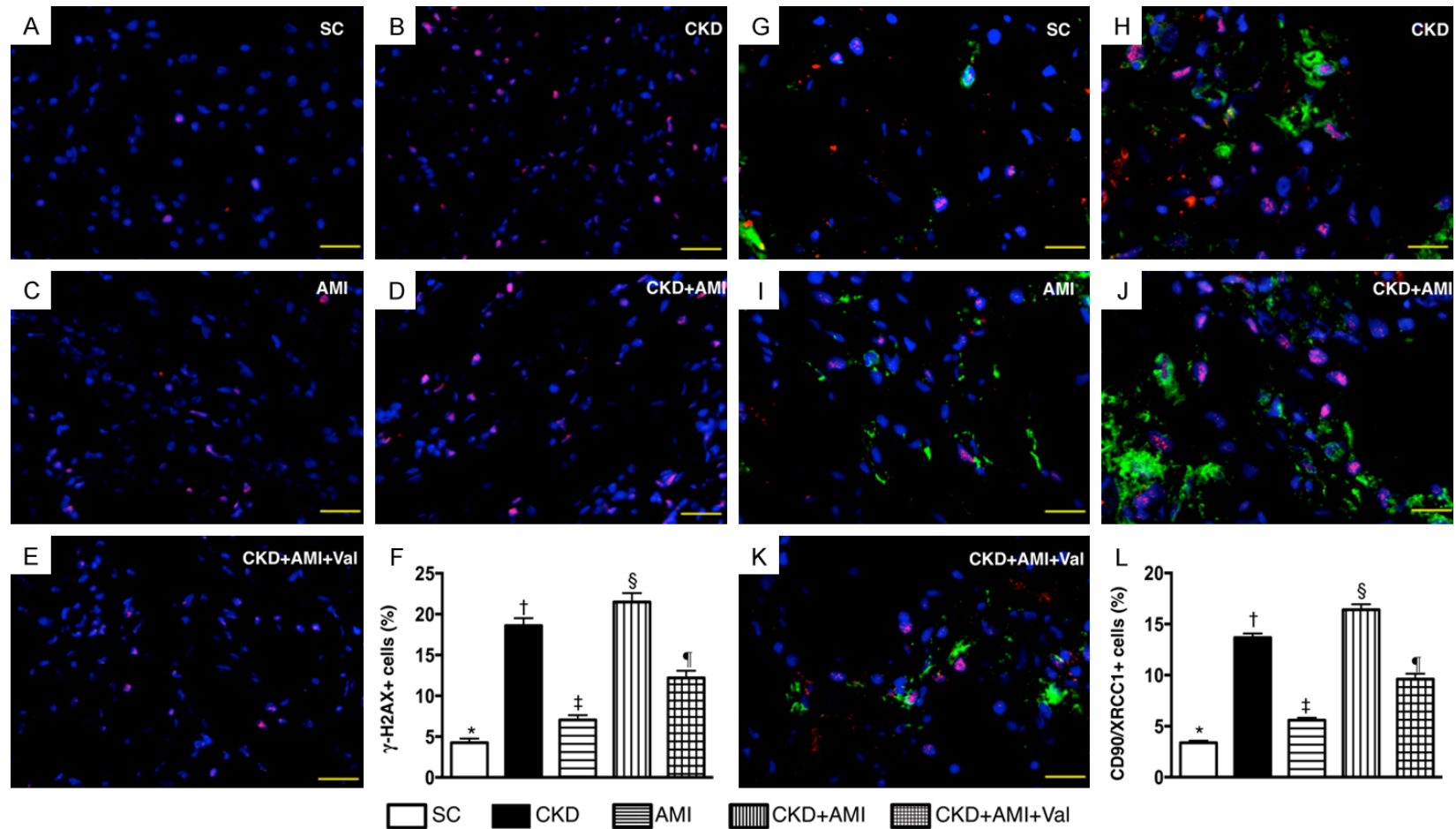


Figure 6. Expressions of γ -H2AX+ cells and XRCC1+/CD cells in Kidney Parenchyma by Day 60 after CKD Induction. A-E. IF microscopic finding (400x) illustrated the γ -H2AX+ cells (pink color). F. Analytical results of γ -H2AX+ cell expression in kidney parenchyma, * vs. other groups with different symbols (†, ‡, §, ¶), $p < 0.0001$. G-K. IF microscopic finding (400x) illustrated the CD90/XRCC1+ cells. Pink color indicated positively stained XRCC1, green color indicated positively stained CD90, positively double stain (i.e., pink and green colors) indicated CD90+/XRCC1+ cells. L. Analytical result of XRCC1+ cells, * vs. other groups with different symbols (†, ‡, §, ¶), $p < 0.0001$. Scale bars in right lower corner represent 20 μ m. All statistical analyses were performed by one-way ANOVA, followed by Bonferroni multiple comparison post hoc test ($n = 10$). Symbols (*, †, ‡, §, ¶) indicate significance (at 0.05 level). SC = sham control; AMI = acute myocardial infarction; CKD = chronic kidney disease; Val = valsartan.

Cardiac function affects CKD & modulated by valsartan

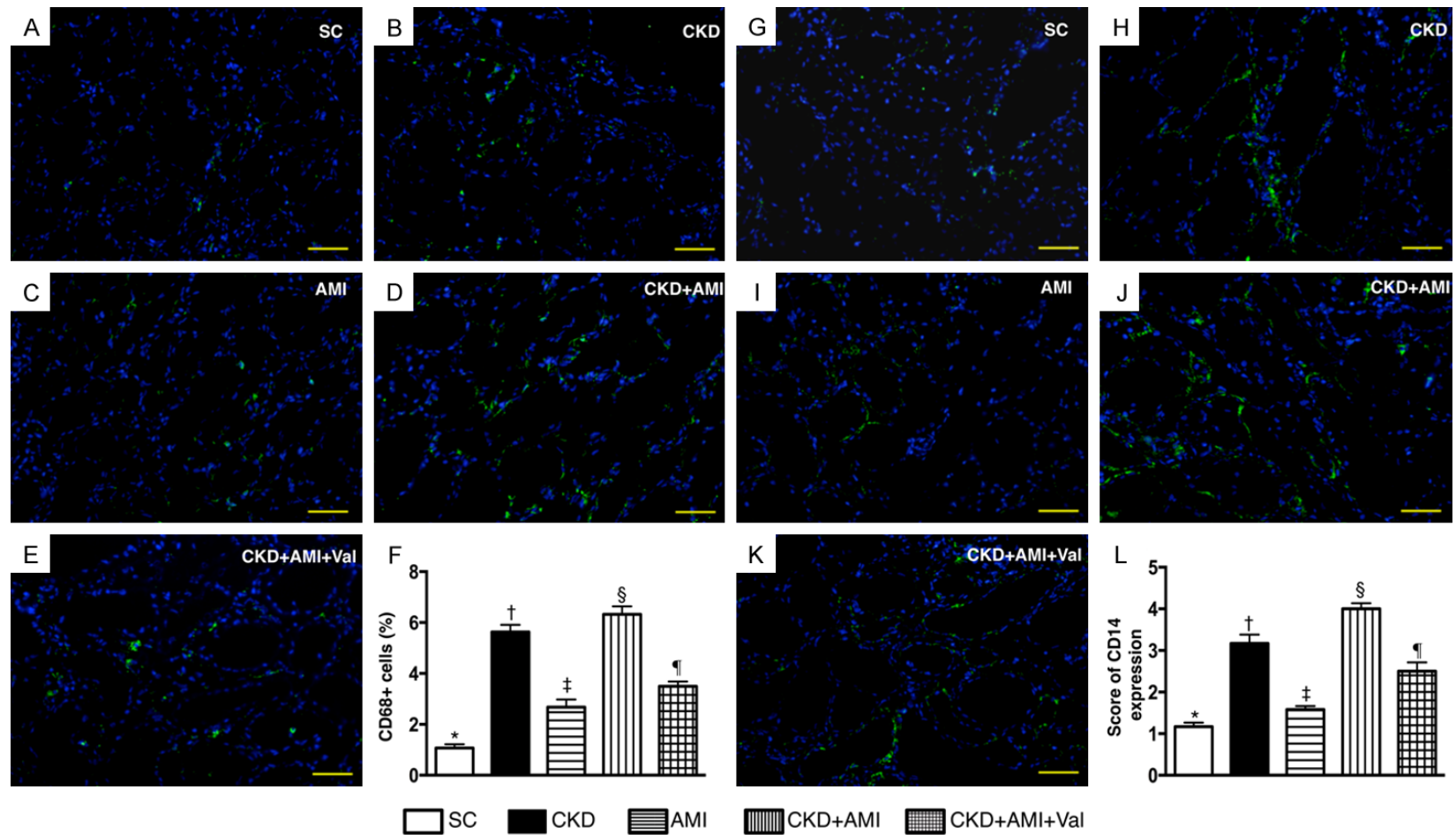


Figure 7. Inflammatory cell infiltration in Kidney Parenchyma by Day 60 after CKD Induction. A-E. IF microscopic finding (400x) of CD68+ cells (green color). F. Analytical results of CD68+ cell expression in kidney parenchyma, * vs. other groups with different symbols (†, ‡, §, ¶), $p < 0.0001$. G-K. IF microscopic finding (400x) of CD14+ cells (green color). L. Analytical results of CD14+ cell expression in kidney parenchyma, * vs. other groups with different symbols (†, ‡, §, ¶), $p < 0.0001$. Scale bars in right lower corner represent 20 μ m. All statistical analyses were performed by one-way ANOVA, followed by Bonferroni multiple comparison post hoc test ($n = 10$). Symbols (*, †, ‡, §, ¶) indicate significance (at 0.05 level). SC = sham control; AMI = acute myocardial infarction; CKD = chronic kidney disease; Val = valsartan.

Cardiac function affects CKD & modulated by valsartan

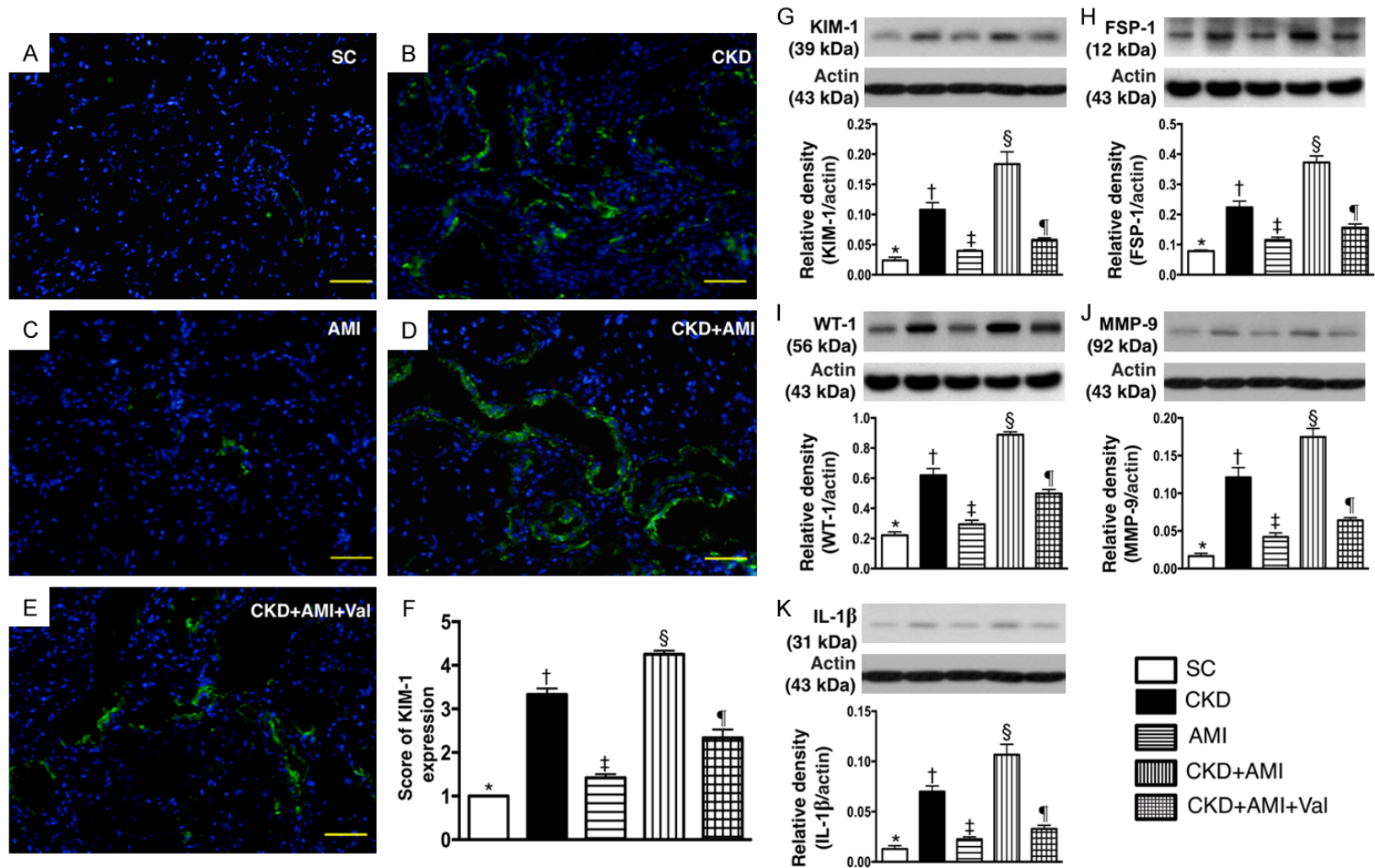


Figure 8. Protein expressions of kidney injury and Inflammation biomarkers in kidney parenchyma by day 60 after CKD induction. A-E. Microscopic finding (400x) of immunofluorescent (IF) stain illustrated kidney injury molecule 1 (KIM-1)+ cells (green color). F. Analytical results of KIM+ cell expression in kidney parenchyma, * vs. other groups with different symbols (†, ‡, §, ¶), $p < 0.0001$. G. Protein expression of kidney injury molecule 1 (KIM-1), * vs. other groups with different symbols (†, ‡, §, ¶), $p < 0.0001$. H. Protein expression of fibroblast specific protein 1 (FSP-1), * vs. other groups with different symbols (†, ‡, §, ¶), $p < 0.0001$. I. Protein expression of Wilm’s tumor suppressor gene 1 (WT-1), * vs. other groups with different symbols (†, ‡, §, ¶), $p < 0.0001$. J. Protein expression of matrix metalloproteinase 9 (MMP-9), * vs. other groups with different symbols (†, ‡, §, ¶), $p < 0.0001$. K. Protein expression of interleukin 1 β (IL-1 β), * vs. other groups with different symbols (†, ‡, §, ¶), $p < 0.0001$. All statistical analyses were performed by one-way ANOVA, followed by Bonferroni multiple comparison post hoc test ($n = 10$). Symbols (*, †, ‡, §, ¶) indicate significance (at 0.05 level). SC = sham control; AMI = acute myocardial infarction; CKD = chronic kidney disease; Val = valsartan.

that provides a link between the integral membrane proteins and the filamentous cytoskeleton in podocytes, was highest in SC and lowest in CKD-AMI, significantly higher in CKD than that in AMI and CKD-AMI-Val, and significantly higher in CKD-AMI-Val than in AMI. Besides, the IHC staining showed that the expression of podocin (**Figure 4**), one component of podocyte foot process, showed a pattern identical to that of ZO-1 among the five groups.

Moreover, IHC analysis also demonstrated that change in the expression P-cadherin (**Figure 5**) which was predominantly located in renal glomerulus exhibited an identical pattern of ZO-1 among all groups. Besides, IF staining demonstrated that synaptopodin (**Figure 5**), one component of podocyte foot process, displayed an identical pattern of expression compared to that of ZO-1 among the five groups.

Cellular expressions of DNA damage biomarkers in kidney parenchyma by day 60 after CKD induction (Figure 6)

IF microscopy of renal parenchyma showed that the numbers of cells positive for γ -H2AX and XRCC1/CD90, two indicators of DNA damage, were highest in CKD-AMI and lowest in SC, significantly higher in CKD than those in the AMI and CKD-AMI-Val groups, and significantly higher in CKD-AMI-Val than those in the AMI group.

Cellular expressions of inflammation markers in kidney parenchyma by day 60 after CKD induction (Figure 7)

If staining of kidney parenchyma revealed that the numbers of cells positively stained for CD68 and CD14, two indices of inflammation, were highest in CKD-AMI and lowest in SC, significantly higher in CKD than those in AMI and CKD-AMI-Val, and significantly higher in CKD-AMI-Val than those in the AMI group.

Cellular and protein expressions of kidney injury and inflammation biomarkers in kidney parenchyma by day 60 after CKD induction (Figure 8)

The cellular and protein expressions of KIM-1, a kidney injury biomarker predominantly expressed in renal tubules, and fibroblast specific protein 1 (FSP-1), predominantly situated in kid-

ney interstitials, were highest in CKD-AMI and lowest in SC, significantly higher in CKD than those in AMI and CKD-AMI-Val, and significantly higher in CKD-AMI-Val than those in AMI. Additionally, the protein expression of Wilm's tumor suppressor gene 1 (WT-1), predominantly located in podocytes, exhibited an identical pattern compared to that of KIM-1 among the five groups. Furthermore, the protein expressions of MMP-9 and IL-1 β , two indicators of inflammation, displayed an identical pattern compared to that of KIM-1 among all groups.

Protein expressions of oxidative stress in kidney parenchyma by day 60 after CKD induction (Figure 9)

The protein expressions of NOX-1 and NOX-2, two indicators of reactive oxygen species (ROS), were highest in CKD-AMI and lowest in SC, significantly higher in CKD than those in AMI and CKD-AMI-Val groups, and significantly higher in CKD-AMI-Val than those in the AMI animals. Additionally, Ang II R-1, an indirect indicator of ROS, displayed a pattern identical to that of NOX-1 among all groups. Furthermore, the expression of oxidized protein, an index of oxidative stress, also showed an identical pattern compared to that of NOX-1 among the five groups.

Protein expressions of apoptotic, fibrotic and anti-fibrotic markers in kidney parenchyma by day 60 after CKD induction (Figure 10)

The protein expressions of cleaved caspase 3 and cleaved PARP, two indicators of apoptosis, were highest in CKD-AMI and lowest in SC, significantly higher in CKD than in those in AMI and CKD-AMI-Val groups, and significantly higher in CKD-AMI-Val than those in AMI animals. Besides, the protein expressions of Smad3 and TGF- β , two indicators of fibrosis, showed an identical pattern compared to that of caspase 3 among the five groups. On the other hand, the protein expressions of Smad1/5 and BMP-2, displayed a pattern opposite to that of caspase 3 among all groups.

Discussion

This study, which investigated the adverse impact of heart dysfunction after AMI on renal function and the therapeutic potential of valsartan therapy against deterioration in renal

Cardiac function affects CKD & modulated by valsartan

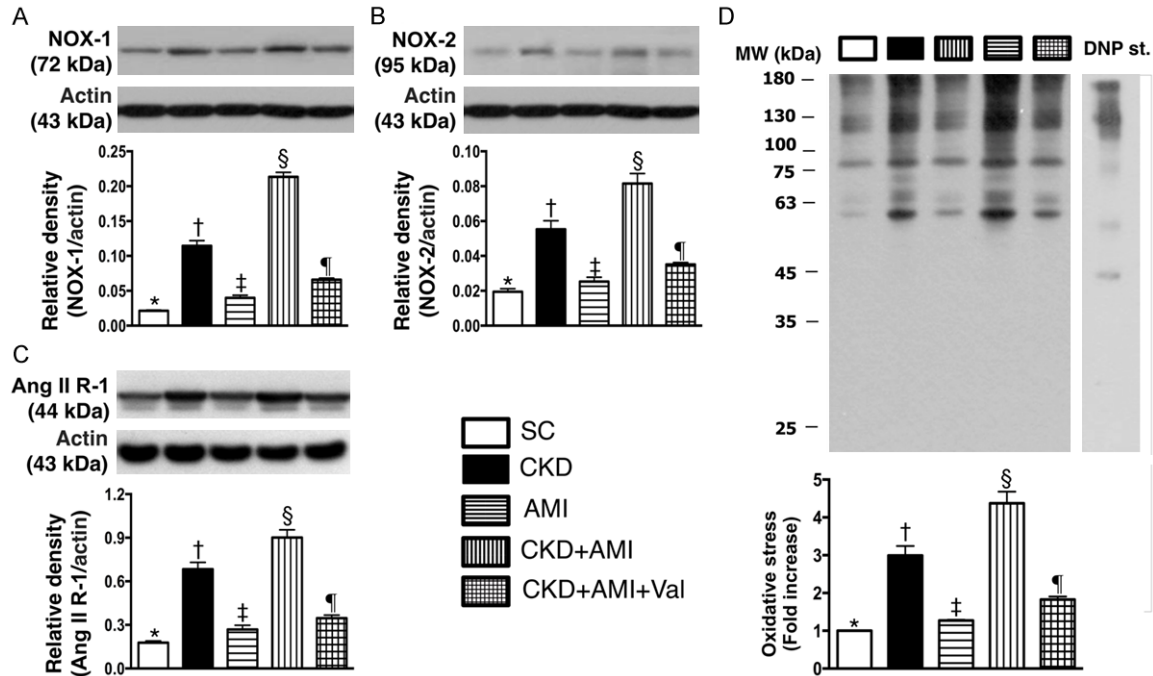


Figure 9. Protein expressions of oxidative stress in kidney parenchyma by day 60 after CKD induction. A. Protein expression of NOX-1, * vs. other groups with different symbols (†, ‡, §, ¶), $p < 0.0001$. B. Protein expression of NOX-2, * vs. other groups with different symbols (†, ‡, §, ¶), $p < 0.0001$. C. Protein expression of angiotensin II receptor 1 (Ang II R-1), * vs. other groups with different symbols (†, ‡, §, ¶), $p < 0.0001$. D. Expression of oxidized protein, * vs. other groups with different symbols (†, ‡, §, ¶), $p < 0.0001$. (Note: the right and left lanes shown on the upper panel represent protein molecular weight marker and control oxidized molecular protein standard, respectively). M.W = molecular weight; DNP = 1-3 dinitrophenylhydrazone. All statistical analyses were performed by one-way ANOVA, followed by Bonferroni multiple comparison post hoc test ($n = 10$). Symbols (*, †, ‡, §, ¶) indicate significance (at 0.05 level). SC = sham control; AMI = acute myocardial infarction; CKD = chronic kidney disease; Val = valsartan.

function in an experimental setting of CKD, yielded several striking implications. First, this study successfully created an animal model for the elucidation of the detrimental renal influence of AMI-induced cardiac dysfunction in the setting of CKD. Second, the results of the present study showed that not only the renal function but also the kidney parenchyma was further impaired when AMI was superimposed on the preexisting CKD. Third, the result of this study proved the concept of organ cross-talk, suggesting that functional impairment of one organ can lead to dysfunction of another. Fourth, valsartan treatment significantly reversed the molecular-cellular perturbations of kidney parenchyma and preserved renal function in the present rodent setting of CKD.

An association between CRS and poor short-term and long-term prognostic outcomes in cardiovascular disease have been fully investigated [10-15]. Intriguingly, while the impact of impaired renal function on the unfavorable

clinical outcome in patients with CVD has been extensively investigated, the influence of impaired heart function on renal function in the CKD setting has infrequently been reported [9-15, 24]. The most important finding in the present study is that, as compared with the CKD animals, the levels of creatinine and BUN as well as the ratio of urine protein to creatinine were remarkably elevated in CKD-AMI animals. Additionally, histopathological analysis demonstrated that the kidney injury score, short axis of kidney that reflected its size, muscularization and thickening renal arterioles were remarkably increased in CKD-AMI animals compared with those in the CKD only animals. On the other hand, the renal blood flow was significantly reduced in CKD-AMI animals compared to that in the AMI only animals. Moreover, this study found that, as compared with SC animals, even in the setting of AMI without preexisting CKD, the renal function and the kidney injury score were still notably impaired in animals with AMI compared with that in the SC

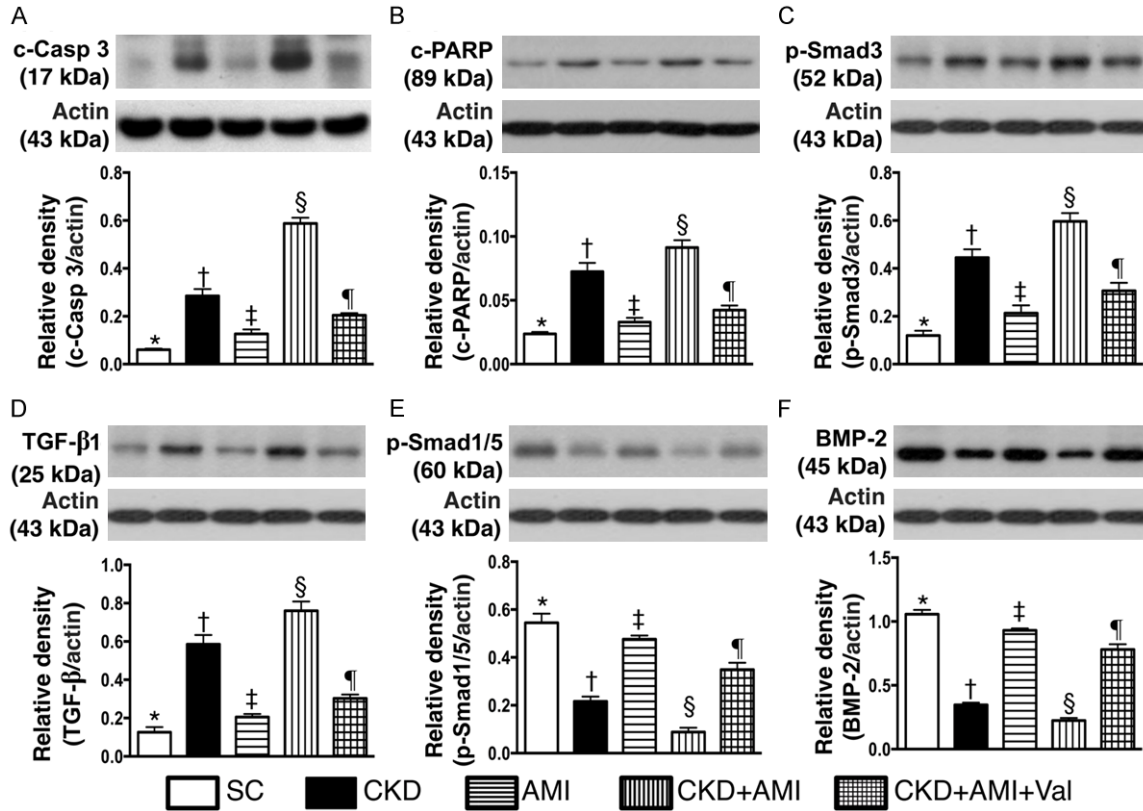


Figure 10. Protein expressions of apoptotic, fibrotic and anti-fibrotic biomarkers in kidney parenchyma by day 60 after CKD induction. A. Protein expression of cleaved caspase 3 (c-Casp 3), * vs. other groups with different symbols (†, ‡, §, ¶), $p < 0.0001$. B. Protein expression of cleaved poly (ADP-ribose) polymerase (c-PARP), * vs. other groups with different symbols (†, ‡, §, ¶), $p < 0.0001$. C. Protein expression of Smad3, * vs. other groups with different symbols (†, ‡, §, ¶), $p < 0.0001$. D. Protein expression of transforming growth factor (TGF)- β , * vs. other groups with different symbols (†, ‡, §, ¶), $p < 0.0001$. E. Protein expression of Smad1/5, * vs. other groups with different symbols (†, ‡, §, ¶), $p < 0.0001$. F. Protein expression of bone morphogenetic protein (BMP)-2, * vs. other groups with different symbols (†, ‡, §, ¶), $p < 0.0001$. All statistical analyses were performed by one-way ANOVA, followed by Bonferroni multiple comparison post hoc test ($n = 10$). Symbols (*, †, ‡, §, ¶) indicate significance (at 0.05 level). SC = sham control; AMI = acute myocardial infarction; CKD = chronic kidney disease; Val = valsartan.

group. Importantly, valsartan treatment markedly preserved the above-mentioned parameters. Therefore, our findings, in addition to strengthening the those of previous studies [9-15, 24], highlighted the crucial role of normal cardiac function in the maintenance of renal function in the setting of preexisting CKD.

Abundant data have shown that acute kidney injury and CKD cause a reduction in podocyte number, density and function, resulting in an impaired glomerular filtration and proteinuria [25-28] which, therefore, can serve as early indicators of renal dysfunction. An essential finding in the present study is that, as compared with SC, protein and cellular expressions of podocyte components were notably

reduced in animals with AMI only, further notably reduced in CKD and even more significantly reduced in CKD-AMI animals. On the other hand, the proteinuria was remarkably increased in those of animals with losing the integrity of podocytes. Our findings, therefore, in addition to reinforcing those of previous studies [25-28], once again demonstrated that heart dysfunction after AMI contributes to the deterioration of renal function in the CKD setting. In fact, not only were the podocyte components substantially reduced in CKD, but the protein and cellular expressions of kidney injury biomarkers (i.e., KIM-1, WT-1, FSP-1) were also increased in a manner opposite to that of podocyte components among all groups of animals. Of particular importance is that the perturbations of

these biomarkers were abrogated after valsartan treatment, suggesting that ARB therapy effectively preserves renal function in CKD setting.

When the pathological findings of diseased renal arterioles were reviewed, the number of muscularized arterioles (i.e., indices of proliferation of smooth muscle layer and reduction in renal perfusion) along with thickness of renal arterioles was significantly increased in the CKD-AMI group than those in the CKD and AMI only animals. On the other hand, the number of small vessels (i.e., an indicator of the integrity of blood perfusion in kidney parenchyma) displayed a reversed pattern of expression compared to that of arteriolar muscularization in kidney parenchyma. Accordingly, these findings, in addition to explaining the markedly reduced blood flow in AMI only animals, further reduction in CKD only animals, and an even more significant decrease in the CKD-AMI group. The results may also explain significant stepwise aggravation of kidney dysfunction and kidney injury score from AMI to CKD-AMI animals. Valsartan treatment, on the other hand, suppressed the progressions of these pathological changes.

Our previous findings have shown that the expressions of inflammation, apoptosis, fibrosis and DNA damage biomarkers were significantly enhanced in rodent models of acute kidney ischemia-reperfusion injury and CKD [18, 20, 21, 28]. A principal finding in the present study is that, as compared with the SC, the cellular and protein expressions of DNA damage, inflammation, fibrosis and apoptosis biomarkers as well as the expression of angiotensin receptor were notably higher in animals with AMI only, further increased in the CKD only group and still further elevated in the CKD-AMI animals. The increases, again, were suppressed after valsartan treatment. Therefore, our findings, in addition to corroborating those of our previous studies [18, 20, 21, 28], underscore the important detrimental influence of heart dysfunction on renal function and the crucial role of valsartan in pharmacomodulation that preserved renal function in an experimental CKD setting.

Study limitation

This study has limitations. First, valsartan was the only IRB drug to be utilized in the present

study. Therefore, this study did not provide the information regarding the impact of the ARBs other than valsartan on protecting the renal function in setting of CKD-AMI. Second, the administration of valsartan was just at day 14 after CKD induction, a timing for early treatment of CKD. Therefore, this study did not provide the answer for whether valsartan treatment was still effective in late stage of CKD for protecting the deterioration of the renal function.

In conclusion, the results of the present study showed that cardiac dysfunction after AMI would aggravate pre-existing kidney dysfunction and impair renal parenchymal integrity in a rodent model of CKD through a series of insults at cellular and molecular levels. On the other hand, the findings of this study demonstrated that valsartan treatment effectively prevented the deterioration in renal function in the present experimental setting, thereby further supporting the current extensive clinical use of angiotensin receptor blockers in CKD patients.

Acknowledgements

This study was supported by a program grant from Chang Gung Memorial Hospital Research Project, Taiwan (Grant number: CMRPG8C1041). We thank the molecular imaging core of the Center for Translational Research in Biomedical Sciences, Kaohsiung Chang Gung Memorial Hospital, Kaohsiung, Taiwan for technical and facility supports on Echo Vevo 2100.

Disclosure of conflict of interest

None.

Address correspondence to: Dr. Jiunn-Jye Sheu, Division of Thoracic and Cardiovascular Surgery, Department of Surgery, Kaohsiung Chang Gung Memorial Hospital and Chang Gung University College of Medicine, 123, Da-Pei Road, Niao-Sung Dist., Kaohsiung 83301, Taiwan. Tel: +886-7-7317123; Fax: +886-7-7322402; E-mail: cvsjjs@gmail.com

References

- [1] Ruddox V, Mathisen M and Otterstad JE. Prevalence and prognosis of non-specific chest pain among patients hospitalized for suspected acute coronary syndrome - a systematic literature search. *BMC Med* 2012; 10: 58.

Cardiac function affects CKD & modulated by valsartan

- [2] Robinson JG, Wallace R, Limacher M, Sato A, Cochrane B, Wassertheil-Smoller S, Ockene JK, Blanchette PL and Ko MG. Elderly women diagnosed with nonspecific chest pain may be at increased cardiovascular risk. *J Womens Health (Larchmt)* 2006; 15: 1151-1160.
- [3] Go AS, Chertow GM, Fan D, McCulloch CE and Hsu CY. Chronic kidney disease and the risks of death, cardiovascular events, and hospitalization. *N Engl J Med* 2004; 351: 1296-1305.
- [4] Raymond NT, Zehnder D, Smith SC, Stinson JA, Lehnert H and Higgins RM. Elevated relative mortality risk with mild-to-moderate chronic kidney disease decreases with age. *Nephrol Dial Transplant* 2007; 22: 3214-3220.
- [5] Coca SG, Yusuf B, Shlipak MG, Garg AX and Parikh CR. Long-term risk of mortality and other adverse outcomes after acute kidney injury: a systematic review and meta-analysis. *Am J Kidney Dis* 2009; 53: 961-973.
- [6] Bydash JR and Ishani A. Acute kidney injury and chronic kidney disease: a work in progress. *Clin J Am Soc Nephrol* 2011; 6: 2555-2557.
- [7] Coca SG, Singanamala S and Parikh CR. Chronic kidney disease after acute kidney injury: a systematic review and meta-analysis. *Kidney Int* 2012; 81: 442-448.
- [8] Chawla LS and Kimmel PL. Acute kidney injury and chronic kidney disease: an integrated clinical syndrome. *Kidney Int* 2012; 82: 516-524.
- [9] Chen YL, Chen CH, Wallace CG, Wang HT, Yang CC and Yip HK. Levels of circulating microparticles in patients with chronic cardiorenal disease. *J Atheroscler Thromb* 2015; 22: 247-256.
- [10] Sadeghi HM, Stone GW, Grines CL, Mehran R, Dixon SR, Lansky AJ, Fahy M, Cox DA, Garcia E, Tchong JE, Griffin JJ, Stuckey TD, Turco M and Carroll JD. Impact of renal insufficiency in patients undergoing primary angioplasty for acute myocardial infarction. *Circulation* 2003; 108: 2769-2775.
- [11] Yamaguchi J, Kasanuki H, Ishii Y, Yagi M, Nagashima M, Fujii S, Koyanagi R, Ogawa H, Hagiwara N, Haze K, Sumiyoshi T, Honda T and Investigators H. Serum creatinine on admission predicts long-term mortality in acute myocardial infarction patients undergoing successful primary angioplasty: data from the Heart Institute of Japan Acute Myocardial Infarction (HI-JAMI) Registry. *Circ J* 2007; 71: 1354-1359.
- [12] Seyfarth M, Kastrati A, Mann JF, Ndrepepa G, Byrne RA, Schulz S, Mehilli J and Schomig A. Prognostic value of kidney function in patients with ST-elevation and non-ST-elevation acute myocardial infarction treated with percutaneous coronary intervention. *Am J Kidney Dis* 2009; 54: 830-839.
- [13] Cardarelli F, Bellasi A, Ou FS, Shaw LJ, Veledar E, Roe MT, Morris DC, Peterson ED, Klein LW and Raggi P. Combined impact of age and estimated glomerular filtration rate on in-hospital mortality after percutaneous coronary intervention for acute myocardial infarction (from the American College of Cardiology National Cardiovascular Data Registry). *Am J Cardiol* 2009; 103: 766-771.
- [14] Koganei H, Kasanuki H, Ogawa H and Tsurumi Y. Association of glomerular filtration rate with unsuccessful primary percutaneous coronary intervention and subsequent mortality in patients with acute myocardial infarction: from the HIJAMI registry. *Circ J* 2008; 72: 179-185.
- [15] Lautamaki A, Kiviniemi T, Biancari F, Airaksinen J, Juvonen T and Gunn J. Outcome after coronary artery bypass grafting and percutaneous coronary intervention in patients with stage 3b-5 chronic kidney disease. *Eur J Cardiothorac Surg* 2016; 49: 926-30.
- [16] Chua S, Sheu JJ, Chang LT, Lee FY, Wu CJ, Sun CK and Yip HK. Comparison of losartan and carvedilol on attenuating inflammatory and oxidative response and preserving energy transcription factors and left ventricular function in dilated cardiomyopathy rats. *Int Heart J* 2008; 49: 605-619.
- [17] Chua S, Chang LT, Sun CK, Sheu JJ, Lee FY, Youssef AA, Yang CH, Wu CJ and Yip HK. Time courses of subcellular signal transduction and cellular apoptosis in remote viable myocardium of rat left ventricles following acute myocardial infarction: role of pharmacomodulation. *J Cardiovasc Pharmacol Ther* 2009; 14: 104-115.
- [18] Huang TH, Chen YT, Sung PH, Chiang HJ, Chen YL, Chai HT, Chung SY, Tsai TH, Yang CC, Chen CH, Chen YL, Chang HW, Sun CK and Yip HK. Peripheral blood-derived endothelial progenitor cell therapy prevented deterioration of chronic kidney disease in rats. *Am J Transl Res* 2015; 7: 804-824.
- [19] Chen YL, Sun CK, Tsai TH, Chang LT, Leu S, Zhen YY, Sheu JJ, Chua S, Yeh KH, Lu HI, Chang HW, Lee FY and Yip HK. Adipose-derived mesenchymal stem cells embedded in platelet-rich fibrin scaffolds promote angiogenesis, preserve heart function, and reduce left ventricular remodeling in rat acute myocardial infarction. *Am J Transl Res* 2015; 7: 781-803.
- [20] Chen YT, Yang CC, Zhen YY, Wallace CG, Yang JL, Sun CK, Tsai TH, Sheu JJ, Chua S, Chang CL, Cho CL, Leu S and Yip HK. Cyclosporine-assisted adipose-derived mesenchymal stem cell therapy to mitigate acute kidney ischemia-reperfusion injury. *Stem Cell Res Ther* 2013; 4: 62.
- [21] Chen HH, Lin KC, Wallace CG, Chen YT, Yang CC, Leu S, Chen YC, Sun CK, Tsai TH, Chen YL,

Cardiac function affects CKD & modulated by valsartan

- Chung SY, Chang CL and Yip HK. Additional benefit of combined therapy with melatonin and apoptotic adipose-derived mesenchymal stem cell against sepsis-induced kidney injury. *J Pineal Res* 2014; 57: 16-32.
- [22] Sun CK, Lee FY, Sheu JJ, Yuen CM, Chua S, Chung SY, Chai HT, Chen YT, Kao YH, Chang LT and Yip HK. Early combined treatment with cilostazol and bone marrow-derived endothelial progenitor cells markedly attenuates pulmonary arterial hypertension in rats. *J Pharmacol Exp Ther* 2009; 330: 718-726.
- [23] Yen CH, Leu S, Lin YC, Kao YH, Chang LT, Chua S, Fu M, Wu CJ, Sun CK and Yip HK. Sildenafil limits monocrotaline-induced pulmonary hypertension in rats through suppression of pulmonary vascular remodeling. *J Cardiovasc Pharmacol* 2010; 55: 574-584.
- [24] Sederholm Lawesson S, Alfredsson J, Szummer K, Fredrikson M and Swahn E. Prevalence and prognostic impact of chronic kidney disease in STEMI from a gender perspective: data from the SWEDEHEART register, a large Swedish prospective cohort. *BMJ Open* 2015; 5: e008188.
- [25] Wiggins RC. The spectrum of podocytopathies: a unifying view of glomerular diseases. *Kidney Int* 2007; 71: 1205-1214.
- [26] Macconi D, Bonomelli M, Benigni A, Plati T, Sangalli F, Longaretti L, Conti S, Kawachi H, Hill P, Remuzzi G and Remuzzi A. Pathophysiologic implications of reduced podocyte number in a rat model of progressive glomerular injury. *Am J Pathol* 2006; 168: 42-54.
- [27] Wharram BL, Goyal M, Wiggins JE, Sanden SK, Hussain S, Filipiak WE, Saunders TL, Dysko RC, Kohno K, Holzman LB and Wiggins RC. Podocyte depletion causes glomerulosclerosis: diphtheria toxin-induced podocyte depletion in rats expressing human diphtheria toxin receptor transgene. *J Am Soc Nephrol* 2005; 16: 2941-2952.
- [28] Yip HK, Yang CC, Chen KH, Huang TH, Chen YL, Zhen YY, Sung PH, Chiang HJ, Sheu JJ, Chang CL, Chen CH, Chang HW and Chen YT. Combined melatonin and exendin-4 therapy preserves renal ultrastructural integrity after ischemia-reperfusion injury in the male rat. *J Pineal Res* 2015; 59: 434-47.